articles

molecular pharmaceutics

Effects of Triton X-100 Nanoaggregates on Dimerization and Antioxidant Activity of Morin

Weiya Liu and Rong Guo*

School of Chemistry and Chemical Engineering, Yangzhou University, Yangzhou 225002, People's Republic of China

Received November 6, 2007; Revised Manuscript Received March 1, 2008; Accepted March 14, 2008

Abstract: Dimerization and antioxidant activity of morin in the Triton X-100 micelles were studied by electronic absorption, ATR-FTIR spectra, cyclic voltammetric, DSC, freeze−fracture TEM, molecular modeling and ab initio quantum calculations. Morin can be solubilized in the Triton X-100 micelles and show selective dimerization in Triton X-100 micelles with different structures. In Triton X-100 spherical micelles, morin always exists in the form of dimer, and in Triton X-100 rodlike micelles, it is always in the form of monomer. The solubilization of morin dimer in Triton X-100 spherical micelles changes the micelle morphology from spherical to cubelike, and the size of the single micelle is also increased, while morin monomer links the Triton X-100 rodlike micelles and forms a kind of network micelle structure with the size of the "rod" unchanged. Solubilized and concentrated in Triton X-100 micelles, morin can protect human serum albumin from the damage induced by hydroxyl radicals effectively and even can form a kind of protein complex with human serum albumin showing more thermal stability.

Keywords: Morin; Triton X-100 micelle; dimerization; HSA; antioxidant activity; hydroxyl radical; ab initio quantum calculation; freeze−fractured TEM; DSC

Introduction

Morin (3,2′,4′,5,7-pentahydroxyflavone; Scheme 1) is one of the most common flavonoids present in nature, which can be found in plant, fruits, flowers and plant derived foods.[1–3] Morin consists of two aromatic rings (A and B in Scheme 1) which are linked by an oxygen-containing heterocycle (ring C). Abundant in the human diet, with potent antioxidant and metal ion chelating capacity, morin possesses various biological and biochemical effects including anti-inflammatory, antineoplastic and cardiprotective activities.[4,5]Potential alternatives to synthetic phenolics being commonly used for the food industry, morin may also have healthy benefits because epidemiological studies already have indicated that adequate intakes of flavonoid-rich foods may reduce the risk of coronary

Scheme 1. The Structure of Morin

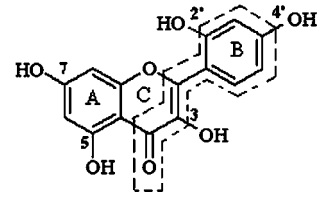

* To whom correspondence should be addressed. Mailing address: Yangzhou University, School of Chemistry and Chemical Engineering, 180 Siwangting Street, Yangzhou, Jiangsu, 225002, People's Republic of China. E-mail: guorong@yzu.edu.cn. Fax: 86-514-7311374. Phone: 86-514-7975219.

(1) Pietta, P. G. Flavonoids as antioxidants. *J. Nat. Prod.* **2000**, *63*, 1035–1042.

(2) Cook, N. C.; Samman, S. Flavonoids-chemistry, metabolism, cardio-protective effects, and dietary sources. *J. Nutr. Biochem.* **1996**, *7*, 66–76.

(3) Harbome, J. B.; Williams, C. A. Advances in flavonoid research since 1992. *Phytochemistry* **2000**, *55*, 481–504.

(4) Middleton, E.; Kandaswami, C.; Theoharides, T. C. The effect of plant flavonoids on mammalian cells: implications for inflammation, heat disease and cancer. *Pharmacol. Rev.* **2000**, *52*, 673–751.

(5) Lee, K. G.; Shibamoto, T.; Takeoka, G. R.; Lee, S. E.; Kim, J. H.; Park, B. S. Inhibitory Effects of Plant-Derived Flavonoids and Phenolic Acids on Malonaldehyde Formation from Ethyl Arachidonate. *J. Agric. Food Chem.* **2003**, *51* (24), 7203–7207.

10.1021/mp7001413 CCC: $40.75
Published on Web 05/30/2008

heart disease and certain cancers.[6–8] The antioxidant properties of morin are directed to scavenge OH•, superoxide anion and highly reactive species implicated in the initiation of lipid peroxidation. On the other hand, as a phenolic compound, the antioxidant effects of morin may act through chelating low valent metal ions such as Fe^{2+} or Cu^{2+} and regenerating membrane bound antioxidants such as α-tocopherol.[9–11] A full understanding of the mode of action of morin, however, requires the study of its interaction with all possible biological targets in a simulated physiological environment.

Self-assemblies of surfactants have attracted great attention in the past two decades, ranging from fundamental areas in biochemistry and physical chemistry to many applicable aspects, such as pharmacology, catalysis, microreactor, and cosmetic. Surfactant molecules in solution can spontaneously assemble into large, stable structures with well-defined geometries, which are closely related to living systems.[12,13] Proteins and other biologically active molecules can be incorporated into a nanoaggregate palisade layer or interior; therefore self-assembly can serve as a model of a biological cell.[13] The solubilization of antioxidants in the different phases and environments of micelles results in different physicochemical interactions compared to homogeneous systems. Many studies have demonstrated that the activity of antioxidants can vary strongly depending on the systems in which they have been solublized.[14–16] For careful study of the location of the antioxidants and therefore to be able to characterize the chemical microenvironment of the antioxidants in micelle solutions, the partitioning behavior[17,18] of antioxidants between the micellar phase and the aqueous phase is crucial for understanding differences in antioxidant activity as a function of surfactant with different charges. The location and the resulting chemical microenvironment of morin were previously studied in micellar solutions using the cationic cetyl trimethyl ammonium bromide (CTAB) and the anionic sodium dodecyl sulfate (SDS). The different charges of the micelles system led to different changes of morin in its molecular planarity, location position, electrostatic component distribution, aggregation state, and eventually led to different levels of its antioxidant ability.[19–21] In these studies, ab initio quantum calculation and molecular optimization were performed to provided a comprehensive description of the molecular structure of morin. The nonionic Triton X-100 micelle system (Scheme 2) was used to model the physiological microenvironment, and the dimerization and antioxidant properties of morin in this system were investigated through combination of several spectroscopic methods as well as calorimetric and microscopic analysis. The morphology change of Triton X-100 micelles upon its interaction with morin was observed through freeze−fractured TEM. Moreover, because of the low toxicity of Triton X-100, we further investigated the protection of morin for human serum albumin (HSA) against the damage of hydroxyl radicals in the Triton X-100 micelle system.

Scheme 2. The Structure of Triton X-100

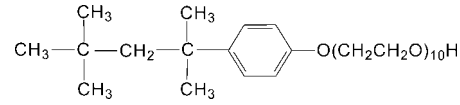

Materials and Methods

Materials. Morin (>99%) was obtained from Merck (Darmstadt, Germany). Triton X-100 (>99%) and pyrene (>99%) were purchased from Sigma-Aldrich Chemical Co (St. Louis, MO). Human serum albumin (>90%) was obtained from Shanghai Biochemical Reagent Company. Hydroxyl radicals were generated by Fenton reagents,[22] and the final Fe^{2+} and H_2O_2 concentrations in the system were 4×10^{-4} and $1 \times$

(6) Yang, C. S.; Landau, J. M.; Huang, M. T.; Newmark, H. L. Inhibition of carcinogenesis by dietary polyphenolic compounds. *Annu. Rev. Nutr.* **2001**, *21*, 381–406.
(7) Hollman, P. C. H.; Hertog, M. G. L.; Katan, M. B. Analysis and health effects of flavonoids. *Food Chem.* **1996**, *57*, 43–46.
(8) Makris, D. P.; Rossiter, J. T. Hydroxyl Free Radical-mediated Oxidative Degration of Quercetin and Morin: A preliminary Investigate. *J. Food. Compos. Anal.* **2002**, *15*, 103–113.
(9) Song, Y.; Kang, J. W.; Wang, Z. H.; Lu, X. Q.; Gao, J. Z.; Wang, L. F. Study on the interaction between CuL_2 and morin with DNA. *J. Inorg. Biochem.* **2002**, *91*, 470–474.
(10) Fang, S. H.; Hou, Y. M.; Chang, W. C.; Hsiu, S. L.; Lee, C.; Pei, D.; Chiang, B. L. Morin sulfates/glucuronides exert anti-inflammatory activity on activated macrophages and decreased the incidence of septic shock. *Life Sci.* **2003**, *74*, 743–756.
(11) Song, Y. M.; Kang, J. W.; Zhou, J.; Wang, Z. H.; Lu, X. Q.; Wang, L. F.; Gao, J. Z. Study on the fluorescence spectra and electrochemical behavior of ZnL_2 and Morin with DNA. *Spectrochim. Acta, Part A* **2000**, *56*, 2491–2497.
(12) Israelachvili, J. *Surfactants in solutions*; Mittal, K. L., Bothorel, P., Eds.; Plenum: New York, 1986.
(13) Fendler, J. H. *Membrane Mimetic Chemistry*; Wiley: New York, 1982.
(14) Sharma, R. In *Surfactant adsorption and surface solubilization*; American Chemical Society: Washington, DC, 1995.
(15) Schwarz, K.; Frankel, E. N.; German, J. B. Partiton behaviour of antioxidative phenolic compounds in heterophasic system. *Fett/Lipid* **1998**, *98*, 115–121.
(16) Stöckmann, H.; Schwarz, K.; Huynh-Ba, T. The influence of various emulsifiers on the partitioning and antioxidant activity of hydroxybenzoic acid and their derivatives in oil-in-water emulsions. *JAOCS* **2000**, *77*, 535–542.
(17) Stöckmann, H.; Schwarz, K. Partitioning of low molecular weight compounds in oil-in-water emulsions. *Langmuir* **1999**, *15*, 6142–6149.
(18) Pekkarinen, S. S.; Stöckmann, H.; Schwarz, K.; Heinonen, M; Hopia, A. I. Antioxidants activity and partitioning of phenolic acid in bulk and emulsified methyl linoleate. *J. Agric. Food Chem.* **1999**, *47*, 3036–3043.
(19) Liu, W.; Guo, R. Interaction between Morin and Sodium Dodecyl Sulfate (SDS) Micelles. *J. Agric. Food Chem.* **2005**, *53*, 2890–2896.
(20) Liu, W.; Guo, R. The Interaction between Morin and CTAB Aggregates. *J. Colloid Interface Sci.* **2005**, *290*, 564–573.
(21) Liu, W.; Guo, R. The Interaction between Flavonoid, Quercetin and Surfactant Aggregates with Different Charges. *J. Colloid Interface Sci.* **2006**, *302* (2), 625–632.
(22) Magnani, L.; Gaydou, E. M.; Hubaud, J. C. Spectrophotometric measurement of antioxidant properties of flavones and flavonols against superoxide anion. *Anal. Chim. Acta* **2000**, *411*, 209–216.

10^{-3}mol/L, respectively. The water used was double-distilled, and the other chemicals were of analytical reagent grade.

Ab Initio Quantum Calculation and Molecular Optimization of Morin. The electronic structure calculations of morin were carried out with the GAUSSIAN 98 program. The single level method used was DFT. The geometries and the vibrational frequencies were obtained at the (U)B3LYP/6-31G(d) level. The final energies were obtained in single-point calculations at the (U)B3LYP/6-311+G(2df,2p) level. For further confirmation, the structure of morin was also built with the MOE software. For each conformation obtained after simple minimization with different force fields, potential energy (PE) was calculated. The force fields used were TAFF, AMBER89, Engh-Huber, MMFF94, CHARMM22, and Empirical Force Field.

UV−Vis Spectral Measurements. Morin was dissolved in the Triton X-100 micelles, and after 1 h of mixing, the spectra were recorded by using UV-240 spectrophotometer (Shimadzu) in the wavelength range 200−500 nm. Distilled water was used as the blank. In the antioxidant experiments, the decay of morin under the attack of the hydroxyl radicals was measured by recording its characteristic peak intensity decrease vs time.

Microenvironment Polarity Measurements. Pyrene, used as probe, was dissolved in Triton X-100/morin mixed solution. Pyrene shows five emission peaks when it is excited at 388 nm. The intensity ratio of the first (at about 373 nm) and the third peak (at about 384 nm) can indicate the polarity of the microenvironment where the pyrene exits. Furthermore, pyrene was used as a probe to detect the location of small molecules (usually the same size) in the micelle system, since the solubilization of other molecules will definitely change the surroundings of the pyrene. As a result, the location of morin in the Triton X-100 micelles can be determined from the change of I_1/I_3 values of pyrene.[23–26]

ATR-FTIR Spectral Measurements. FTIR spectra of morin in the Triton X-100 micelles were recorded with a Brucker Equinox 55 FT-IR spectrometer. Single-beam IR spectra were the result of about 64 coadded interferograms with a ZnSe ATR optical accessory set at 45° used as a reflectance medium. The FTIR spectra range from 400 to 2000 cm^{-1} with a spectral resolution of 4 cm^{-1}. For each measurement, the program automatically subtracted the signal of the Triton X-100 micelles which was used as the blank.

Determination of the Voltammetric Properties of Morin. Cyclic voltammetric experiments of morin were carried out with CH Instruments 660a electrochemical workstation (Zhenghua, Shanghai). A glassy carbon electrode was used as the working electrode (3.0 mm diameter), a platinum electrode worked as the auxiliary electrode, and a saturated calomel electrode was used as the reference electrode. The solutions were prepared in acetic acid−sodium acetate buffers, and the exact pH values of the system (ranging from 4.4 to 5.6) were determined by PHs-25 pH-meter (Leizi Instrumental Factory, Shanghai).

Differential Scanning Calorimetry. Calorimetric experiments were performed with Netzsch DSC-204 F1. DSC thermograms of HSA were obtained from 25 to 100 °C at a scan rate of 1.5 °C/min. A protein concentration of 0.75 mg/mL at the appropriate pH 7.4 was employed. A baseline correction was performed by subtracting the results of a sample versus buffer thermogram under identical conditions.

Transmission Electron Microscopy Measurements. A TECNAI-12 TEM (Philips) transmission electron microscopy was used to detect the morphology and size change of Triton X-100 micelle upon its interaction with morin by the freeze−fractured method (BAF 400 D, Balzers, Germany). The damage to HSA (0.75 mg/mL, pH 7.4) induced by the hydroxyl radicals was also investigated by TEM using the negative stain and freeze−fractured methods.

Results and Discussion

Molecular Optimization of Morin by Ab Initio Quantum Calculation and Molecular Operating Environment. Morin possesses hydroxyl groups at the 2′ and 4′ positions on the B-ring, which are the most potent parts to scavenge the free radicals in the molecule (Scheme 1). Ab initio quantum calculation showed that the most stable conformation of morin molecule is not planar. The B-ring in the morin molecule is connected to the C-ring by a single C−C bond around which rotation can occur, and the B-ring deviates by 38.98° from planarity (Figure 1). The optimized conformation of morin molecule was further analyzed with the MOE software, and similar results were obtained; B-ring, the most active part of the morin molecule, is not in the same planarity as the rest of the morin molecule.

Selective Dimerization of Morin in Triton X-100 Micelles of Different Structures. The UV absorbance of morin at room temperature in aqueous solution manifests a maximum at about 375 nm, which is associated with the light absorption of the cinnamyl system, the frame part of the morin molecule in Scheme 1 including the 2′, 4′ hydroxyl groups. The transition is $\pi-\pi^*$ in nature, and can be represented by the resonance structures depicted as follows:

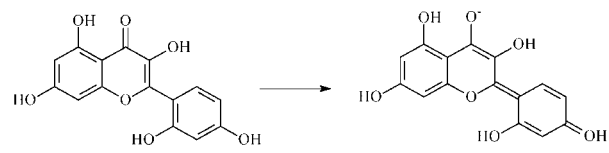

(23) Kalynasundaram, K.; Thaomas, J. K. Environmental effects on vibronic band intensities in pyrene monomer fluorescence and their application in studies of micellar systems. *J. Am. Chem. Soc.* **1977**, *99*, 2039–2044.
(24) Guo, R.; Yu, W.; Zhang, X. Effect of VC on the phase behavior of surfactant system. *Acta Phys.-Chim. Sin.* **2000**, *16*, 325–330.
(25) Liu, W.; Guo, R.; Guo, X. Isomerization of Malachite Green in CTAB/n-$C_nH_{2n+1}OH/H_2O$ Mixed Micelles. *J. Dispersion Sci. Technol* **2003**, *24* (2), 219–228.
(26) Guo, R.; Liu, W.; Fan, G. K. Interaction of Malachite Green with CTAB micelles. *Acta Phys.-Chim. Sin.* **2001**, *17* (12), 1062–1067.
(27) Liu, R. T.; Yang, J. G.; Wu, X.; Hua, S.; Sun, C. X. Interaction of morin with CTMAB: aggregation and location in micelles. *Spectrochim. Acta, Part A* **2001**, *57*, 2561–2566.
(28) Liu, W.; Guo, R. Interaction of Flavonoid, Quercetin with Molecular Organized Assemblies of Nonionic Surfactant. *Colloids Surf., A* **2006**, *274*, 192–199.

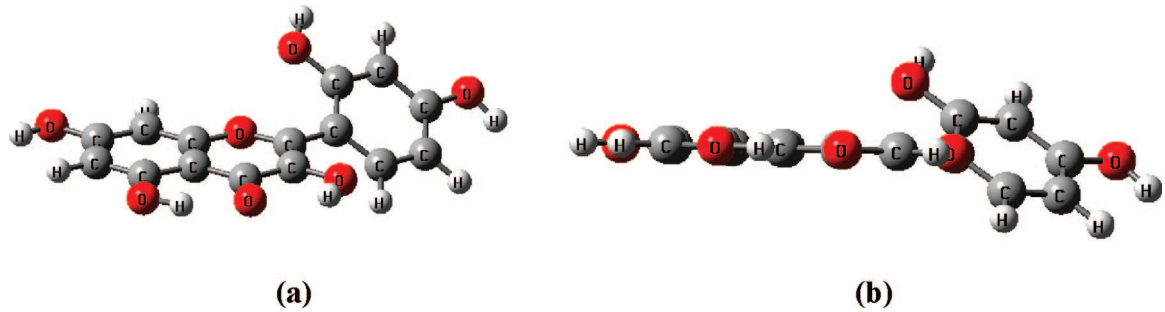

Figure 1. Optimized structure of morin molecule: (a) above view, (b) side view.

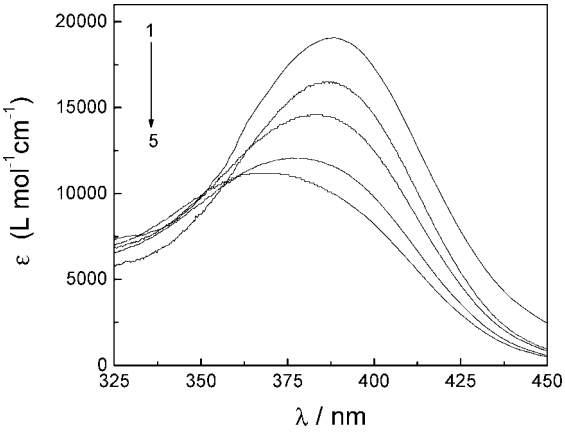

Figure 2. Molar extinction coefficient (ϵ) versus wavelength of morin with increased concentration. Concentration of morin (mol/L): (1) 1.0×10^{-5}, (2) 2.5×10^{-5}, (3) 4.0×10^{-5}, (4) 7.5×10^{-5}, (5) 1.0×10^{-4}.

The relationship between the molar extinction coefficient (ϵ) and wavelength of morin with different concentrations is shown in Figure 2. With morin's concentration increased from 0.01 mM to 0.1 mM, the ϵ_{max} of morin undergoes hypochromic shift from 390 nm to 370 nm, and when the content arrives at 0.1 mM, morin will form the dimer in the aqueous solution.[27] As we know, with increasing concentration, Triton X-100 self-aggregates can change from premicelle (before cmc1), to spherical micelle (after cmc1: 3.2×10^{-4} mol/L), and to rodlike micelle (after cmc2: 1.3×10^{-3} mol/L).[28] Figure 3 represents the absorption spectra of morin in Triton X-100 micelles with different structures. When the original form of morin is monomer (4.0×10^{-5} mol/L), Triton X-100 premicelles only increase its peak intensity (curve 2 in Figure 3a). Triton X-100 spherical micelles cause morin's absorption peak to shift from 390 nm to 370 nm and the peak intensity decreased (curve 3 in Figure 3a), while Triton X-100 rodlike micelles make morin's absorption peak move back to 390 nm and the peak intensity increased (curve 4 in Figure 3a).

When morin is in the form of a dimer (1.0×10^{-4} mol/L), Triton X-100 premicelles cause its absorption peak shifting from 370nm to 390nm with intensity increased (curve 2 in Figure 3b), Triton X-100 spherical micelles cause its absorption peak to shift back to 370 nm with the intensity decreased (curve 3 in Figure 3b); while in Triton X-100 rodlike micelles, the absorption peak of morin returns to 390 nm (curve 4 in Figure 3b). The UV results show that no matter whether the morin is in the form of monomer or dimer, when solubilized in Triton X-100 spherical micelles, it prefers to stay in the form of a dimer (with the absorption peak at 370 nm), and when solubilized in Triton X-100 rodlike micelles, it always exists in the form of a monomer (with the absorption peak at 390 nm). In the aqueous solution, morin mainly exists in the anionic state with one or two negative charges,[27] while Triton X-100 is a kind of nonionic surfactant, the electrostatic interaction between them can be ignored. Due to the aromatic rings within the molecular structure, morin is predominately located in the micellar phase and not in the aqueous phase in both Triton X-100 spherical and rodlike micelles, so the "concentration effect" could not explain the selective dimerization of morin well. The nanoscale solubilization spaces provided by the Triton X-100 micelles of different structures might be a possible reason for this selective dimerization. As we can see from the scheme below: with the micellar structure changing from spherical then to rodlike, Triton X-100 molecules arrange more compactly and tightly in the micelles, which makes the available solubilization space decreased. It is reasonable to assume that, due to the limited solubilization space of the Triton X-100 rodlike micelles, it is difficult for morin to remain in the form of a dimer as in the spherical micelles and thus leads to the selective dimerization of morin.

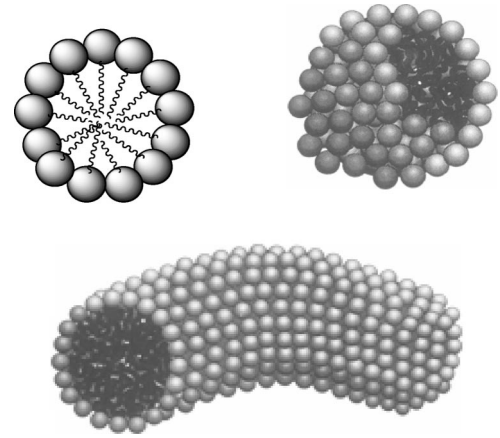

Location of Morin in Triton X-100 Micelles. Molecular optimization of morin molecule indicates that the B-ring of morin deviates by 38.98° from the planarity of the rest of the molecule (Figure 1). To make clear which part of the morin molecule prefers to interact with Triton X-100 micelles is of great importance to the understanding of its location in the Triton X-100 micelles. ATR-FTIR spectroscopy was employed to investigate the interaction site of morin with Triton X-100 micelles. The ATR-FTIR spectra of free morin and morin solubilized in the Triton X-100 micelles are shown

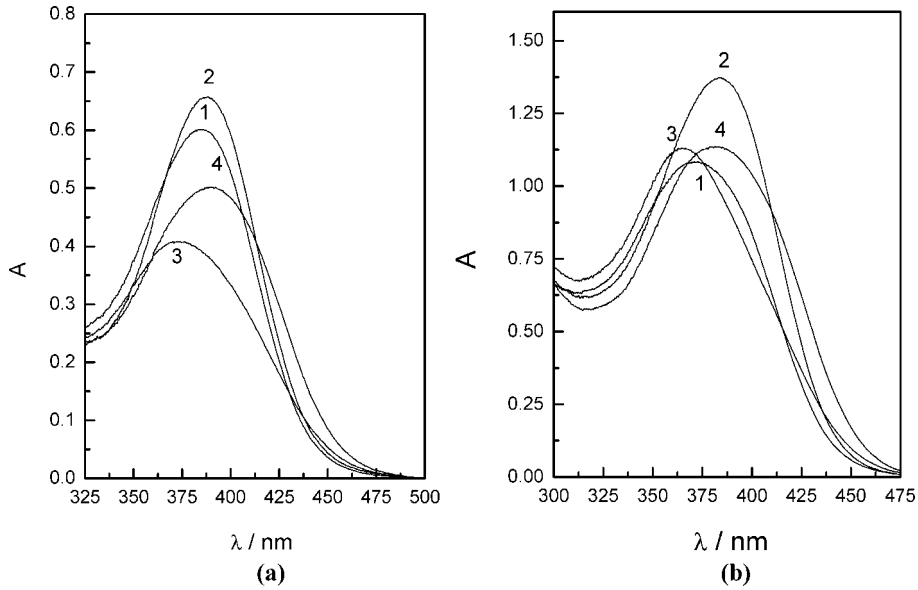

Figure 3. Absorption spectra of morin in Triton X-100 micelles of different structures. Triton X-100 (mol/L): (1) 0.0, (2) 2.0×10^{-5}, (3) 8.0×10^{-4}, (4) 4.0×10^{-3}. Morin (mol/L): (a) 4.0×10^{-5} monomer, (b) 1.0×10^{-4} dimer.

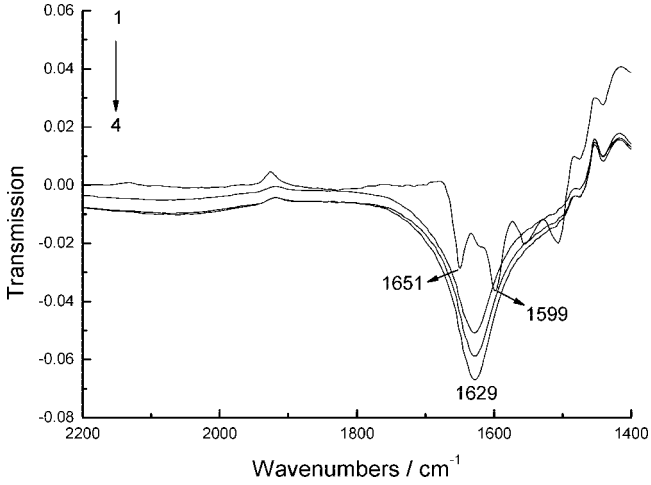

Figure 4. ATR-FTIR spectra of morin (1.0×10^{-2} mol/L) in Triton X-100 micelles. Triton X-100 (mol/L): (1) 0.0, (2) 4.0×10^{-4}, (3) 8.0×10^{-4}, and (4) 2.0×10^{-3}.

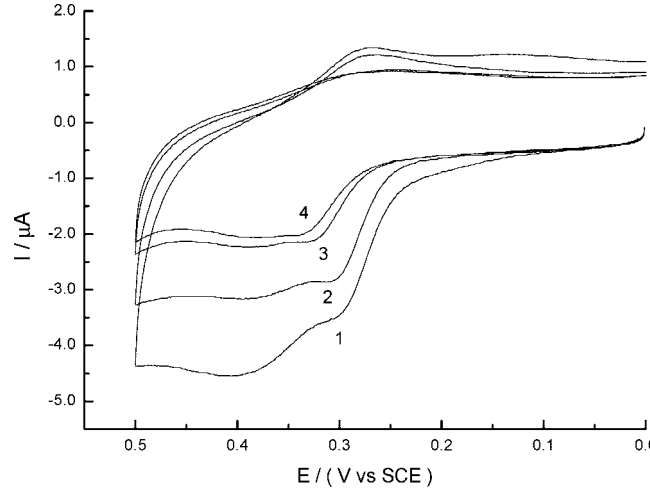

Figure 5. Cyclic voltammograms of morin mixed with different Triton X-100 micelles in acetic acid−sodium acetate (0.2 mol/L) buffer with pH being 5.0. Scan rate: 200 mV.s^{-1}. Triton X-100 (mol/L): (1) 0.0, (2) 2.0×10^{-5}, (3) 8.0×10^{-4}, (4) 2.0×10^{-3}.

in Figure 4 with the spectra ranging from 1400 to 2200 cm^{-1}. For free morin molecule, the two bands located at 1651 and 1596 cm^{-1} are the stretching vibration of C═O and phenyl skeleton, respectively (curve 1 in Figure 4). The original ν (C═O) band of free morin is centered at 1651 cm^{-1}, which is the expectant result of the coupling between C═O and C═C stretching in morin molecule. With solubilization in the Triton X-100 micelles, the ν (C═O) band of morin shifts to a lower frequency with increased intensity, and the ν (C═O) band even covers the phenyl skeleton stretching vibration at 1599 cm^{-1} and eventually forms a broad band centered at 1629 cm^{-1} (curves 2−4 in Figure 4), which indicates the extension of π conjugation and the increase of the planarity of the whole morin molecule.[29] The ATR-FTIR analysis indicates the extension of π conjugation and the increase of the planarity of the whole morin molecule, which supports the conclusion that morin mainly interacts with Triton X-100 micelles through its B-ring part. With the B-ring interacting with Triton X-100 micelles, the rotation of C−C single bond linking B-ring and the rest of the molecule is limited, thus the planarity of the whole morin molecule is increased, which eventually leads to the above change of the molecule vibration in the morin molecule.

Cyclic voltammetry studies were performed to further investigate which part within the morin molecule prefers to interact with Triton X-100 micelles. In the acetic acid−sodium acetate buffer, morin would show a pair of peaks at approximately 0.3 V (curve 1 in Figure 5), which correspond to the redox of 2′, 4′ hydroxyls on the B-ring. The peak currents of morin are linearly dependent on the scan rate,

(29) Xue, Q. *The spectrum methods in the structure study of the macromolecule*; High Education Press: Beijing, PCR, 1995; p 26.

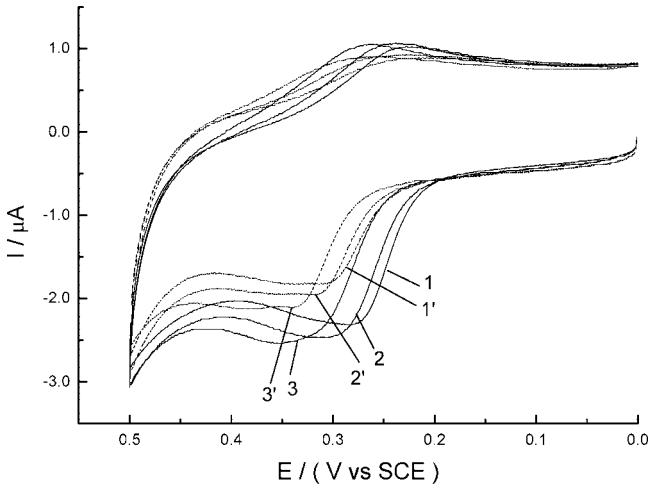

Figure 6. Cyclic voltammograms of morin in the absence (solid line) and the presence (dashed line) of Triton X-100 micelles (8.0×10^{-4} mol/L) at various pH values: (1) pH 5.6, (2) pH 5.4, and (3) pH 5.0. Scan rate: 200 mV s^{-1}.

which indicates that the electrode reaction of morin is a reversible surface electrochemical reaction, with both the reactant and the product strongly absorbed on the electrode surface.[30] The redox of 2′, 4′ hydroxyls on the B-ring within morin molecule is a two-electron and two-proton electrode reaction shown as follows:[31]

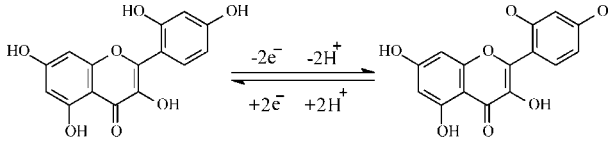

With the addition of Triton X-100 micelles, the oxidant peak of morin moves to a higher potential with decreased peak current (curves 2−4, in Figure 5), which reflects that the 2′, 4′ hydroxyl groups are embedded to a more hydrophilic environment with the B-ring part of morin solubilized in the Triton X-100 micelles. The redox of morin under different pH values with the presence of Triton X-100 micelles were also performed to further test our hypothesis on morin's interaction site (Figure 6). It can be seen from Figure 6 that, though the oxidant peak of morin moves to a lower potential with the increase of the pH values, the oxidant peaks of morin in Triton X-100 micelles all shift to higher potential under each fixed pH value. Both cyclic voltammograms and ATR-FTIR spectroscopy studies show that the interacting site of morin molecule with the Triton X-100 micelles involves the B-ring part.

The location of morin in the Triton X-100 micelles will affect its functionality of antioxidants toward radicals. Pyrene was employed as the probe to obtain insight into the microenvironment of Triton X-100 micelles in which morin exists in our studies. By using ^{1}H NMR method, Schwarz and co-workers[32] demonstrated that the antioxidant propyl gallate (PG) would be located in different regions within the micelles of different charges. In their studies, PG is located in the region of the polyoxyethylene chain of Brij 85 nonionic micelles and still has the ability to diffuse freely within the Brij micelle. Our studies show that morin is mainly located in the palisade layer of Triton X-100 micelles and before Triton X-100 micelles change to rodlike structure, morin molecules do have the freedom to move inside the Triton X-100 micelles.

Table 1. I_1/I_3 Values of Triton X-100 Micelles with Addition of 0, 2.0, and 4.0×10^{-5} M Morin

		micropolarity I_1/I_3		
Triton X-100 (mol/L)	micelle structure	0	2.0	4.0
2.0×10^{-5}	premicelle	1.55	1.62	1.70
4.0×10^{-4}	spherical	1.49	1.58	1.67
8.0×10^{-4}	spherical	1.41	1.50	1.59
4.0×10^{-3}	rodlike	1.23	1.24	1.24

From Table 1, we can see that the I_1/I_3 value of pyrene decreases from 1.55 to 1.23 with increasing Triton X-100 micelle concentration, which indicates that the polarity of the microenvironment of pyrene is decreased with the micelle structure changing from spherical to rodlike. The addition of morin into Triton X-100 micelles of different structures also leads to the change of I_1/I_3 value, which on the other hand can indicates the location of morin within the micelles.[24–26] When morin is added to Triton X-100 spherical micelles, the I_1/I_3 values increase from 1.49 to 1.67; when morin is added to Triton X-100 rodlike micelles, the I_1/I_3 values remain almost unchanged (from 1.23 to 1.24). Above observations indicate that morin might be located at more hydrophobic part of the palisade layer (more closer to the micelle core) in Triton X-100 spherical micelles, but only can be solubilized at less hydrophobic part of the palisade layer (outsides of the palisade layer) in Triton X-100 rodlike micelles. As discussed above, the loose structure and relatively large solubilization space of Triton X-100 spherical micelles allow morin molecules to be located in the form of dimer. As a result, once morin dimer is solubilized in Triton X-100 spherical micelles, the spaces between TritonX-100 molecules are increased and the pyrene molecules tend to be squeezed to the less hydrophobic part of the micellar palisade, so the microenvironment polarity of pyrene is increased and thus leads to the increased value of I_1/I_3 (Table 1). On the contrary, the compact structure and the limited solubilization room of Triton X-100 rodlike micelles only allow the existence of morin monomer and do not permit morin to go deeper into the palisade layer of the rodlike micelles; consequently, the position of pyrene remains unchanged and so does the I_1/I_3 value (Table 1).

(30) Falkovskaia, E.; Sengupta, P. K.; Kasha, M. Photophysical induction of dual fluorescence of quercetin and related hydroxyflavones upon intermolecular H bonding to solvent matrix. *Chem. Phys. Lett.* **1998**, *297*, 109–114.

(31) Zhu, Z. W.; Li, C.; Li, N. Q. Eletrochemical studies of quercetin interacting with DNA. *Microchem. J.* **2002**, *71*, 57–63.

(32) Heins, A.; Sokolowski, T.; Stöckmann, H.; Schwarz, K. Investigating the location of propyl gallate at surfaces and its chemical microenvironment by ^{1}H HMR. *Lipids* **2007**, *42*, 561–572.

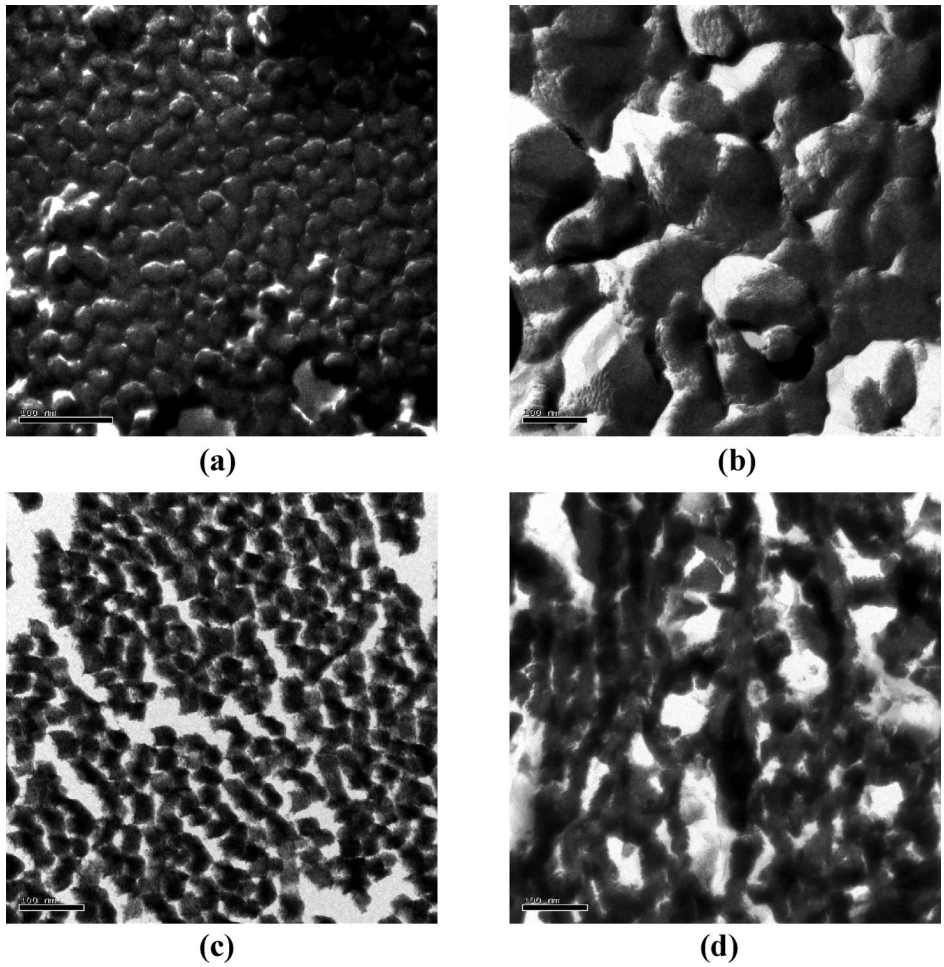

Figure 7. Freeze−fractured images of Triton X-100 micelles with solubilization of morin. Triton X-100 (mol/L): (a, b) 4 × 10^{-4}, (c, d) 2 × 10^{-3}; morin (mol/L): (a, c) 0.0, (b, d) 1 × 10^{-4}.

Morphology Change of Triton X-100 Micelles with Solubilization of Morin. Our previous studies showed that the presence of the flavonoids almost has no influence on cmc1 and cmc2 values of the Triton X-100 micelle. Cmc1 is the concentration above which Triton X-100 will change from premicelles to spherical micelles (3.2 × 10^{-4} mol/L), and cmc2 is the concentration above which the Triton X-100 micelle will change from spherical to rodlike (1.3 × 10^{-3} mol/L).[33]

The morphology changes of Triton X-100 micelles upon interaction with morin were examined by transmission electron microscopy with the freeze−fractured method (Figure 7). At lower Triton X-100 concentration (4 × 10^{-4} mol/L), the structure of Triton X-100 micelles is spherical, which can be can be seen clearly in Figure 7a. With the solubilization of morin, the morphology of micelles is changed from spherical to cubelike and the size of the single micelle is also increased (Figure 7b). With increased concentration (2 × 10^{-3} mol/L), Triton X-100 micelles turn from spherical to rodlike. From Figure 7c, we can observe the existence of rodlike micelles ranged in very high order. With the addition of morin, Triton X-100 rodlike micelles turn to some network structure with the link between rods observed easily, but the size of the "rod" remains the same (Figure 7d). According to previous discussion, we know that morin mainly exists in Triton X-100 spherical micelles in the form of a dimer and can be located at the more hydrophobic part of the palisade layer, which accounts for the increased size and changed morphology of the Triton X-100 spherical micelles. In the case of Triton X-100 rodlike micelles, morin mainly exists in the form of a monomer and is located at the less hydrophobic part of the palisade layer, so morin monomer is possible to link the Triton X-100 rodlike micelles to form a network structure but keep the micelle size unchanged.

Antioxidant Activity of Morin in the Triton X-100 Micelles and Protection of HSA against Hydroxyl Radical-Induced Damage. The antioxidant and the free-radical-scavenging capabilities of morin mainly lie in its ability to function as reducing reagent and terminator of radicals by rapid donation of one or two hydrogen atoms to the radicals.[34]

2′, 4′ two hydroxyl groups on the B-ring are the most active antioxidant parts in the morin molecule, which can scavenge

(33) Guo, R.; Wei, P.; Liu, W. Combined antioxidant effects of rutin and Vitamin C in Triton X-100 micelles. *J. Pharm. Biomed. Anal.* **2007**, *43*, 1580–1586.

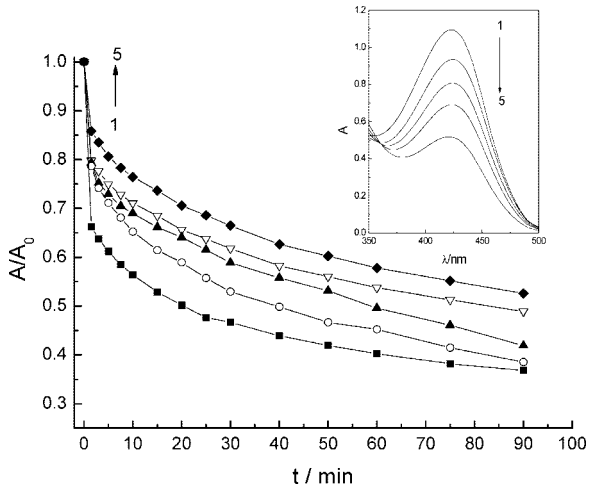

Figure 8. Degradation of morin upon attack by hydroxyl radicals in different Triton X-100 micelles. Triton X-100 (mol/L): (1) 0.0, (2) 4.0×10^{-4}, (3) 8.0×10^{-4}, (4) 2.0×10^{-3}, (5) 4.0×10^{-3}. Inset: Absorption spectra of morin at different time reacted with hydroxyl radicals. Time on the arrow is ordinal 2, 10, 30, 50, 75 min; Triton X-100 (mol/L): 4.0×10^{-3}.

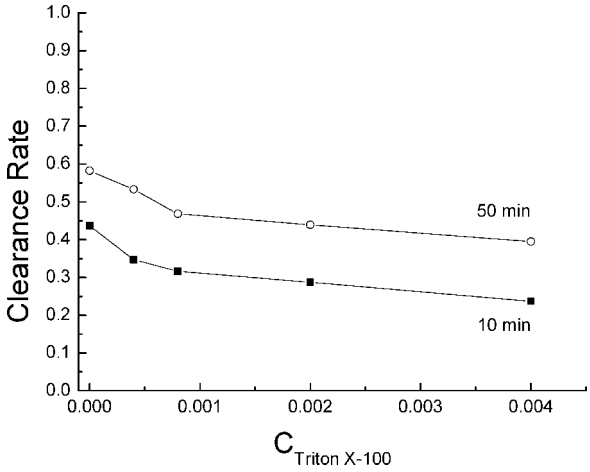

Figure 9. The influence of Triton X-100 micelles on morin's clearance rate of hydroxyl radicals.

hydroxyl radicals. With the hydroxyl radicals cleared, the morin molecule itself will degrade and its absorption peak intensity will decrease accordingly. Therefore, we analyzed morin's ability to scavenge hydroxyl radicals generated by Fenton reagents in the Triton X-100 micelles by measuring its characteristic UV−vis spectroscopy.

$$Fe^{2+} + H_2O_2 \rightarrow Fe^{3+} + \cdot OH + OH^-$$

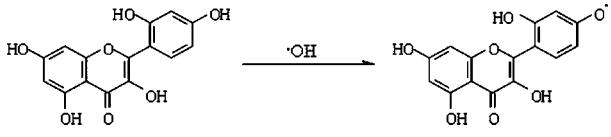

The influence of the Triton X-100 spherical and rodlike micelles on the decay of morin upon attack of hydroxyl radicals is shown in Figure 8. After mixing with Fenton reagents, the absorption peak of morin drops rapidly within

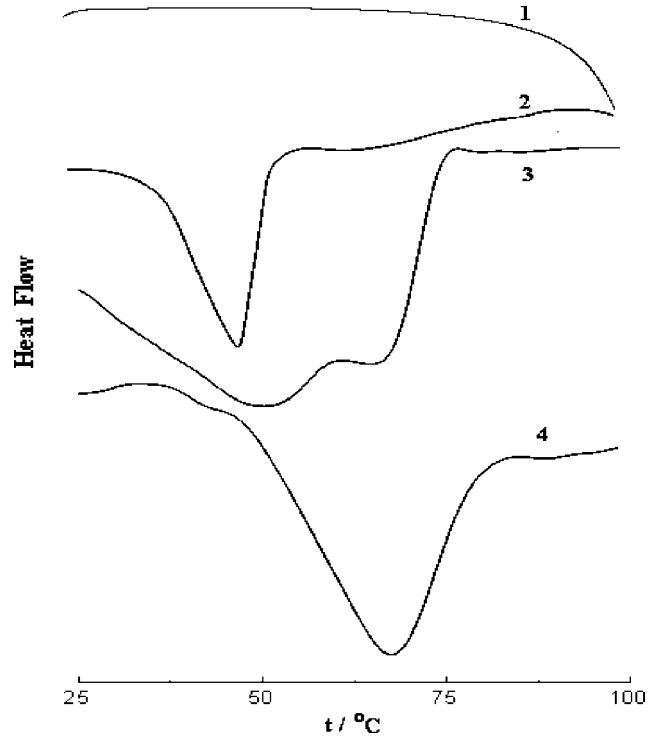

Figure 10. DSC thermograms of thermal denaturation of HSA at pH 7.4. Heating rate: 1.5 K/min. HSA concentration: 0.75 mg/mL, (1) HSA + ·OH, (2) HSA, (3) HSA + ·OH + morin (1×10^{-4} mol/L) + Triton X-100 (4.0×10^{-4} mol/L), (d) HSA + ·OH + morin (1×10^{-4} mol/L) + Triton X-100 (4.0×10^{-3} mol/L).

the first ten minutes, and then this downtrend slows down; when the time attains fifty minutes, the whole downtrend levels off. The reason for this is that, at the beginning of the reaction, there are a great many hydroxyl radicals in the system, which are capable of degrading morin easily and quickly, but with the reaction going on, the amount of hydroxyl radical decreases, and so does the chance of the hydroxyl radicals to attack morin molecules.

Assuring that the amount of hydroxyl radicals is in excess, the A/A_0 ratio of morin could represent its clearance rate for hydroxyl radicals. We measured this clearance rate at ten and fifty minutes in different Triton X-100 micelles respectively (Figure 9). From Figure 9 we can see that, whether at ten or fifty minutes, the clearance rates are both decreased with the increased Triton X-100 micelle concentration, which means that the reaction between morin and hydroxyl radicals is partly blocked with the solubilization of morin within Triton X-100 micelles.

In order to evaluate the influence of Triton X-100 micelles on the antioxidant ability of morin, we compared the ability of morin in protecting HSA from the damage induced by hydroxyl radicals in Triton X-100 micelles of different structures. The thermal denaturation of HSA upon the attack of hydroxyl radicals and those with the protection of morin in different Triton X-100 micelles was investigated by

(34) Rice, E. C. Plant polyphenols: free radical scavengers or chain-breaking antioxidants. *Biochem. Soc. Symp.* **1995**, *61*, 103–116.

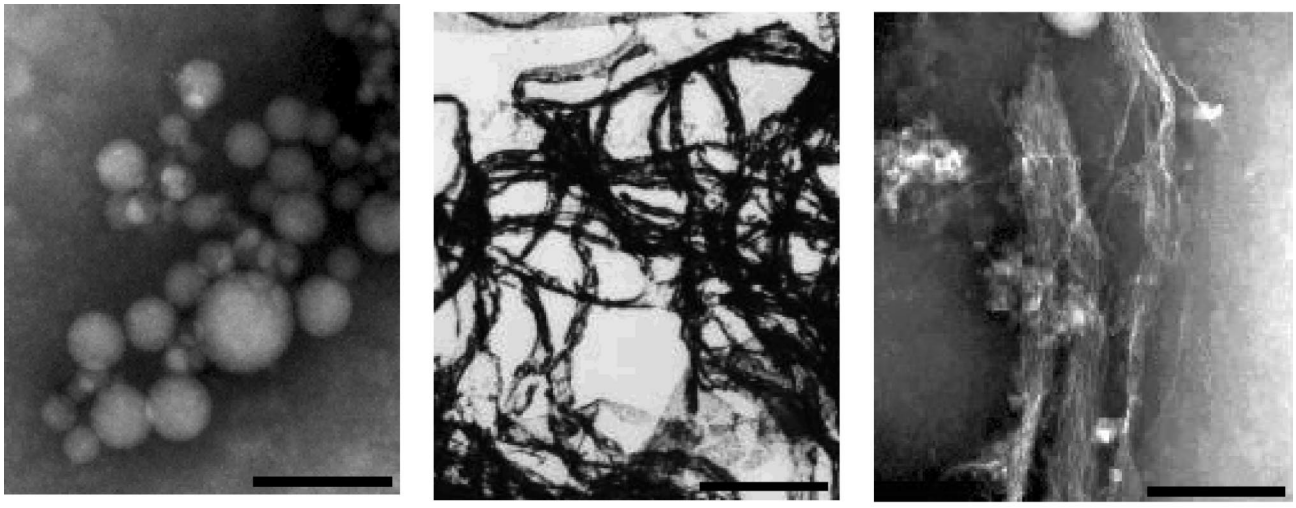

(a) (b) (c)

Figure 11. TEM images of human serum albumin. HSA concentration: 0.75 mg/mL, pH = 7.4. (a) HSA, (b) HSA + ·OH, (c) HSA + ·OH + morin (1×10^{-4} mol/L) + Triton X-100 (4.0×10^{-4} mol/L), the bar on the graph denotes 0.5 μm.

differential scanning calorimetry. As we know, the denaturation of protein causes an endothermic peak in the thermogram;[35] in the case of HSA, the calorimetric scan in the buffer of pH 7.4 is characterized by a single peak centered at about 48 °C (curves 2 in Figure 10). After one hour reaction with hydroxyl radicals, the thermal scan of HSA does not show any peak (curve 1 in Figure 10), which indicates the irreversible damage exerted on the protein by the hydroxyl radicals. With the presence of morin in the Triton X-100 spherical micelles, mixed with hydroxyl radicals, the characteristic peak of HSA at 48 °C appears again but becomes less pronounced, while a new endothermic peak centered at about 68 °C shows at the same time (curve 3 in Figure 10). In the Triton X-100 rodlike micelles, the original peak of HSA at 48 °C totally disappears, while the peak at 68 °C which represents the denaturation of morin−HSA complex manifests (curve 4 in Figure 10). It is obvious that this morin−HSA complex is more thermally stable than the original protein with the denature temperature 20 °C higher than the HSA.

To further evaluate the antioxidant activity of morin in the Triton X-100 micelles and its protection of HSA against the hydroxyl radicals induced damage, the morphology changes of HSA were investigated by TEM (Figure 11). From Figure 11 we can see that the structure of HSA changes from the spherical (Figure 11a) to a completely random intertwist (Figure 11b) without the protection of morin; while in the presence of morin solubilized in Triton X-100 micelles, only some of the HSA are damaged and changed to the random intertwisting morphology, and some of the HSA have been well protected and retain the original structure (Figure 11c).When morin molecules are solubilized in some system with different phases or compartments (such as in blood), its antioxidant ability would change greatly compared to being in the homogeneous aqueous solutions. How does this antioxidant ability alter according to the change of morin's local surroundings? The simulation of the physiological environment by the Triton X-100 micelles has given us some information on this aspect. In general, the morin monomer will possess more capability to scavenge the free radicals than the dimer, but our studies show that this is not always true. When morin is solubilized in the Triton X-100 rodlike micelles in the form of a monomer, its hydroxyl radical clearance rate decreases 20% compared to the aqueous solutions. There are several reasons for this: first, morin molecules interact with Triton X-100 micelles mainly through its B-ring part, with this most potent free radical-scavenging part shielded by the micelle palisade, morin's antioxidant activity will be decreased undoubtedly. Second, when solubilized in the Triton X-100 rodlike micelles, morin will change the Triton X-100 micelles from rodlike structure to network, and this network structure of the micelles will inhibit the collision between morin molecules and hydroxyl radicals and reduce morin's antioxidant activity consequently.

Conclusions

The present study demonstrates that morin can be solubilized in the Triton X-100 micelles and show selective dimerization with the Triton X-100 micelle structure change. Whether the original form of morin is monomer or dimer, in the Triton X-100 spherical micelles it is always in the form of a dimer while in the Triton X-100 rodlike micelles it is in the form of a monomer. The microenvironment difference of morin inside the Triton X-100 spherical and rodlike micelles is investigated by using pyrene as the probe. The clearance of hydroxyl radicals by morin and the protection of human serum albumin against hydroxyl radical induced damage by morin have been investigated in the Triton X-100 micelles by UV, DSC and TEM. In the Triton X-100 micelles, morin can protect human serum

(35) Privalov, P. L.; Khechinashvili, N. N. A thermodynamic approach to the problem of stabilisation of globular protein structure: A calorimetric study. *J. Mol. Biol.* **1974**, *86*, 665–684.

albumin from the damage induced by hydroxyl radicals effectively, and can form a morin−HSA complex which is more thermally stable than the original protein with the denature temperature 20 °C higher. Furthermore, our studies find that morin dimer will change the morphology of Triton X-100 micelles from spherical to cubelike and increase the size of the single micelle, while the morin monomer will link the Triton X-100 rodlike micelles and form a kind of network micelle structure with the size of the "rod" unchanged.

Acknowledgment. This research work was supported by the National Nature Science Foundations of China (No. 20633010 and 20773106).

Supporting Information Available: Details of the molecular modeling of morin. This material is available free of charge via the Internet at http://pubs.acs.org.

MP7001413